International Journal of Electrical, Electronic and Communication Sciences
ISSN: 2517-9438
Vol:9, No:9, 2015

The Design, Development, and Optimization of a Capacitive Pressure Sensor Utilizing an Existing 9 DOF Platform

Andrew Randles, Ilker Ocak, Cheam Daw Don, Navab Singh, Alex Gu

***Abstract*—**Nine Degrees of Freedom (9 DOF) systems are already in development in many areas. In this paper, an integrated pressure sensor is proposed that will make use of an already existing monolithic 9 DOF inertial MEMS platform. Capacitive pressure sensors can suffer from limited sensitivity for a given size of membrane. This novel pressure sensor design increases the sensitivity by over 5 times compared to a traditional array of square diaphragms while still fitting within a 2 mm x 2 mm chip and maintaining a fixed static capacitance. The improved design uses one large diaphragm supported by pillars with fixed electrodes placed above the areas of maximum deflection. The design optimization increases the sensitivity from 0.22 fF/kPa to 1.16 fF/kPa. Temperature sensitivity was also examined through simulation.

***Keywords*—**Capacitive pressure sensor, 9 DOF, 10 DOF, sensor, capacitive, inertial measurement unit, IMU, inertial navigation system, INS.

I. Introduction

MANY areas of consumer, medical and industrial applications a 9 degrees of freedom (9 DOF), 3 axis accelerometer, 3 axis gyroscope and 3 axis magnetometer, systems are used. By adding a pressure sensor to a 9 DOF system it will improve navigation by adding the ability to detect barometric pressure, which would be an indication of the elevation of the sensor. These pressure sensors can also be used in other industrial applications such as pipeline inspection tools, or areas where an integrated inertial sensor system and pressure sensor could be put together such as medical tracking.

Pressure sensors can be based on four different sensing principals, piezoresistive, resonant, optical and capactive detection [1]. All of these methods have different advantages and disadvantages. For piezorestive they are simple to fabricate, only diffused piezoresistors and a diaphragm are needed to fabricate the sensor. These devices have been commercialized by many companies today. They suffer from limited temperature range and temperature sensitivity. Resonant beam sensors can have a wide temperature range, however they can be complicated to fabricate and require specialized circuit for detection. Other examples of pressure sensors include sensors that make use of changes in resonant frequency or time delay of acoustic wave devices such as surface acoustic wave or LAMB wave devices [2]. The acoustic wave based sensors are not applicable here because a piezoelectric layer is not available in this platform. Optical sensors can be very sensitive by monitoring the displacement of the diaphragm. Integration of optical sensors into a 9DOF system would be problematic for a mass produced system.

In the design of capacitive pressure sensors there is a tradeoff between the size of the device, the sensitivity and the static capacitance. A sensor with a higher sensitivity for a given static capacitance will have a larger chip size compared to a device with a lower sensitivity but the same static capacitance. Some improvement of the sensitivity and the chip size can be achieved by optimizing the fixed electrode and moving electrode dimensions and shape. Capacitive sensors have low thermal drift but a small signal and parasitic capacitance in the packaging needs to be addressed.

In the Institute of Microelectronics (IME) a monolithic CMOS compatible 9DOF process has been developed [3]. Many of the needed process modules have been characterized and initial structures have been fabricated. With the structure it is also possible to add a monolithic capacitive pressure sensor to the platform. The entire sensor stack could be bonded to an application specific IC which would reduce the parasitic capacitance in the system. This paper examines the design of the capacitive pressure sensor by optimizing the design to achieve better sensitivity and also examines the temperature dependence of the structure.

II. Fabrication of the Pressure Sensor

The fabrication platform for the 9 DOF has been discussed in a previous paper [3]. It is included here for completeness.

A. Process

The process to realize the pressure sensors on the mentioned 9DOF inertial measurement platform is summarized below. Figs. 1 (a)-(c) show the MEMS wafer which starts with 20 μm deep cavity etching on the handle layer. It is followed with buried oxide (BOX) growth, fusion bonding and thinning the device layer of the cavity SOI wafer to 20 μm. Metal and via layers are formed using via last dual damascene process. The primary reason to fabricate these metal and via layers are to build magnetic coil structures for magnetometers.

Approximately 2 μm thick dielectric is containing the Cu lines is then patterned and used as a hard mask to etch the 20 μm thick device layer underneath. This final DRIE step

A. Randles, I. Ocak, Cheam D.D., N. Singh and A. Gu is with the Institute of Microelectronics, A*STAR (Agency for Science, Technology and Research), Singapore 116875 (Phone: +65-6770-5466; Fax: +65-6774-54747; e-mail: randlesab@ime.a-star.edu.sg).

suspends all the inertial sensors with the help of the cavity underneath them and completes the fabrication of the MEMS wafer. In the case of the pressure sensors the device layer is not etched and cavity is left sealed under high vacuum.

TSI wafer fabrication shown in Figs. 1 (d)-(g) starts with via etching, liner oxide growth on the inner walls, and filling with highly doped n++ epi-poly silicon. It is followed by grinding extra poly-silicon and then front side Al redistribution layer (RDL) fabrication. The wafer was then thinned down to 300 µm from backside to reveal TSVs and then followed by deposition of the spacers, RDL and getter on the backside of the wafer. The Process was completed by bonding MEMS to TSI wafer using Al\Ge bonding (5). Fig. 2 shows an image of the pressure sensor before TSI vacuum packaging, fabricated using the 9DOF inertial MEMS platform.

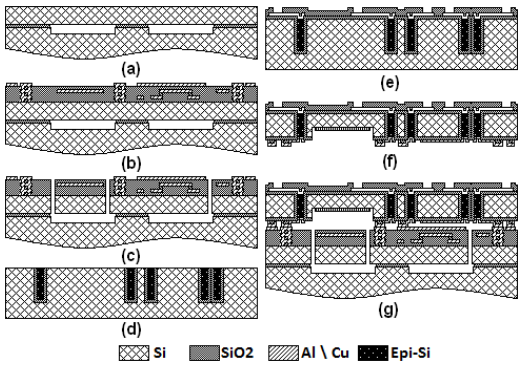

Fig. 1 MEMS wafer (a) cavity wafer (b) 3 metal and via layer deposition (c) structural etch (d) TSI etch and filling (e) Front side RDL and pad etch (f) grinding, stand-off, getter & back RDL (g) Bonded TSI & MEMS wafer bonding [3]

TABLE I
SILICON MATERIAL PROPERTIES FOR UNROTATED SI [4]

elastic constants, c_{ij} [GPa]	c_{11}	164
	c_{12}	64
	c_{44}	80
1st order TCE Tc_{ij} [10^{-6}/K]	Tc_{11}	-73.25
	Tc_{12}	-91.59
	Tc_{44}	-60.14
2nd order TCE $T2c_{ij}$ [10^{-9}/K^2]	$T2c_{11}$	-49.26
	$T2c_{12}$	-32.70
	$T2c_{44}$	-51.28

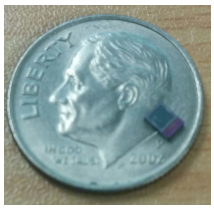

Fig. 2 Fabricated MEMS chip

III. SIMULATION SETUP

The basic layers of the simulation are shown in Fig. 3. The structure is made up of the silicon diaphragm which is also acting as the ground layer in the structure. An air cavity with a moving mesh is the next layer with a variable pressure. Finally the active electrodes are defined above the moving mesh layer. The opposite side of the diaphragm is at vacuum. So the pressure load is applied at the interface between the moving mesh and the Si diaphragm. The vacuum sealed cavity under the moving diaphragm is at 50 mBar. This is set by the fabrication process.

For the Si layer an anisotropic material model was used for the Si that included temperature dependent coefficients for the Si stiffness contestants, Table I. In the simulation software the stiffness matrix was rotated by 45 degrees to align with the XY axis in a (100) wafer. Simulations were done over a range of pressures and temperature to capture the change in sensitivity as a function of pressure.

Many capacitive pressure sensors are designed where the capacitive plates are on either side of the sealed cavity, for example [5]. The proposed design has one disadvantage compared to these other sensors because the atmosphere between the electrodes will change as the outside air changes. This can be accounted for by adding reference capacitors.

TABLE II
DIMENSIONS USED IN SIMULATIONS

Chip Size	2mm x2mm
Maximum distance for unsupported diaphragm	<0.4 mm
Si Thickness	20µm
Air Gap	2µm
Pillar Size	50 µm
Target Static Capacitance	1.67 pF

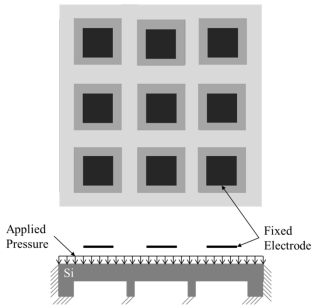

Fig. 3 Standard capacitive sensor setup with multiple diaphragms

IV. SENSITIVITY OPTIMIZATION

A. Square Diaphragms

In the fabrication platform that was used for this pressure sensor, the design constraints for the sensor were a 2 mm x 2 mm square with the largest unsupported diaphragm 0.4 mm x 0.4 mm. The designed static capacitance was set to 1.67 pF. Other details can be found in Table II. A series of simulations were run, where the top electrode size was varied and the number of diaphragms was increased to match the desired static capacitance. An example of the deflection pattern for a square diaphragm is shown in Fig. 4.

Next, a series of simulations were run where the static capacitance was held constant, and the coverage of the top electrode was varied. The sensitivity is plotted in Fig 5.

Fig. 4 Deflection of a single square diaphragm, 0.4 mm x 0.4 mm Contour lines mark the deflection of the diaphragm in µm. The central square marks where the top electrode would be located

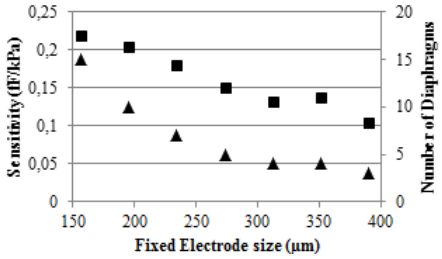

Fig. 5 Sensitivity of the set of diaphragms for different amounts of fixed electrode coverage, the sensitivity of the array of diaphragms is calculated from the sensitivity of one diaphragm times the closest integer of diaphragms

The maximum number of diaphragms was capped at 16 as this is the maximum number that would fit within the 2 mm square. The sensitivity was calculated from the sensitivity of a single diaphragm multiplied by the number of diaphragms that would be required to meet the static capacitance.

B. Optimized Diaphragm Design

To address the low sensitivity of the fully fixed membrane an alternative design using multiple pillars to support the membrane and the active electrode is designed to be placed only over the areas of maximum deflection. The structure is shown in Fig. 6.

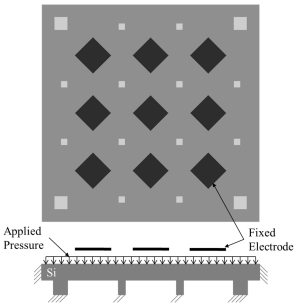

Fig. 6 Layout of an optimized sensor

The total size of the diaphragm was limited to 1.7 mm by 1.7 mm to leave space around the edge for bonding and dicing. The electrodes were set to 200 µm on a side. Simulations of the deflection and sensitivity were performed. The deflection pattern of the device is shown in Fig. 7.

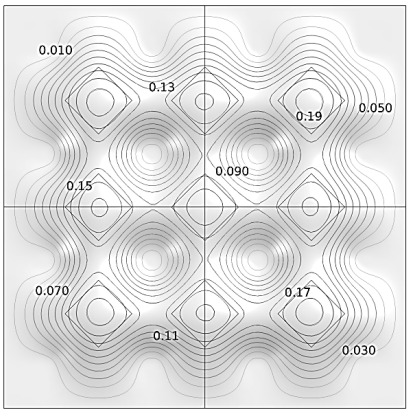

Fig. 7 Deflection of the optimized membrane 1.7 mm x 1.7 mm, contour lines marks the deflection of the diaphragm in µm. The diamonds represent where the fixed electrode is located.

The sensitivity from the optimized structure is 1.16 fF/kPa, more than 5 times increase over the best device shown in Fig. 5. As can be seen in Fig. 4 some further optimization could be done on the electrode shape for them to better follow the contour lines.

C. Temperature Sensitivity of the Optimized Design

The temperature sensitivity of the sensor is critical for determining the error in the sensor and for accounting for the temperature drift. One way to address some of the temperature drift would be to add reference capacitors to the system. Reference capacitors would account for changes in the permittivity of air due to temperature and humidity changes. These capacitors could be placed around the diaphragm edges where there is very little deflection. This will only leave the changes in the Si stiffness as a function of temperature as the main environmental variable not accounted for.

The temperature sensitivity of the optimized diaphragm was studied by using a stiffness matrix that included temperature dependence for Si, Table I. In Fig. 8 is a plot of the sensitivity as a function of temperature.

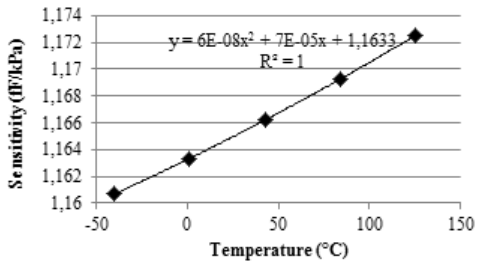

Fig. 8 Sensitivity as a function of temperature for the optimized structure, the sensitivity is changed by 57 ppm/K for the first order effect and 52 ppb/K^2 for the second order dependence

The temperature sensitivity could be reduced by making use of the oxide layer which already exists in the platform. This would likely reduce but not completely eliminate the temperature drift of the sensor. The remaining temperature drift would need to be accounted for in signal processing.

V. Conclusion

In this paper a simulation of an optimized capacitive pressure sensor was developed. The sensor showed a more than 5 times improvement of the sensitivity over a traditional array of Si diaphragms with a similar static capacitance and chip area. The temperature sensitivity of the structure was also simulated.

References

[1] W. P. Eaton and J. H. Smith. "Micro machined pressure sensors: review and recent developments." In *Smart Structures and Materials' 97,* 1997, pp. 30-41.

[2] P. Kropelnicki, K. Muckensturm, X. J. Mu, A. B. Randles, H. Cai, W. C. Ang, J. M. Tsai and H. Vogt. "CMOS-compatible ruggedized high-temperature Lamb wave pressure sensor." *Journal of Micromechanics and Micro-engineering*, vol. 23, no. 8, 2013, pp. 085018.

[3] I. E. Ocak, D. D. Cheam, S. N. Fernando, A. T. Lin, P. Singh, J. Sharma, G. L. Chua, B. Chen, A.Y.D. Gu, N. Singh, and D. L. Kwong "A monolithic 9 degree of freedom (DOF) capacitive inertial MEMS platform." in *Electron Devices Meeting (IEDM), 2014 IEEE International*. San Francisco, 2014, pp. 22-6.

[4] M. Hopcroft, W. D. Nix, and T. W. Kenny. "What is the Young's Modulus of Silicon?" *Micro-electromechanical Systems, Journal of*, vol. 19, no. 2, 2010, pp. 229-238.

[5] M. Narducci, L. Yu-Chia, W. Fang, and J. Tsai. "CMOS MEMS capacitive absolute pressure sensor." *Journal of Micromechanics and Micro-engineering*, vol. 23, no. 5, 2013, pp. 055007.